

Electron-capture-delayed fission properties of ²³⁴Am

H. L. Hall,* K. E. Gregorich, R. A. Henderson, C. M. Gannett,† R. B. Chadwick,
J. D. Leyba, K. R. Czerwinski, B. Kadkhodayan, S. A. Kreek, D. M. Lee,
M. J. Nurmia, and D. C. Hoffman

Nuclear Science Division, Lawrence Berkeley Laboratory, 1 Cyclotron Road, Berkeley, California 94720

C. E. A. Palmer and P. A. Baisden

Nuclear Chemistry Division, Lawrence Livermore National Laboratory, Livermore, California 94550

(Received 7 August 1989)

Delayed fission following the electron-capture decay of ²³⁴Am was studied. The ²³⁷Np(α,7n)²³⁴Am reaction with multiple ²³⁷Np targets was used to produce ²³⁴Am. The fission properties and half-life of ²³⁴Am were measured using a rotating-wheel system. The half-life of ²³⁴Am was determined to be 2.32±0.08 min from measurements of the fission activity. A highly asymmetric mass-yield distribution was observed for the fission activity, and the average total kinetic energy of the fission fragments was found to be 173±5 MeV. Radiochemical separations confirmed the elemental assignment of the fissioning species to americium or fission from short-lived excited states in its EC daughter, plutonium. The cross section for ²³⁴Am produced by this reaction and decaying by electron capture was determined to be 5.4±1.3 μb by measuring the intensities of the daughter plutonium K x rays in radiochemically separated americium samples. The branching ratio of the 6.46-MeV α peak of ²³⁴Am was found to be (3.9±1.2)×10⁻⁴ in on-line measurements. The delayed-fission probability was determined to be (6.6±1.8)×10⁻⁵ from the measured ratio of fissions to plutonium K x rays. The observed fissions were unambiguously assigned to an EC-delayed fission process by measuring fissions coincident with the K-capture x rays.

I. INTRODUCTION

Delayed fission (DF) is a nuclear decay process in which a decaying nucleus populates excited states in its daughter nucleus, which then fission. These states can be above the fission barrier(s) of the daughter (yielding prompt fission), within the second well of the potential energy surface (a fission shape isomer), or within the first well of the potential energy surface (an electromagnetic isomer). This decay mode is believed to influence the production yields of heavy elements in multiple neutron capture processes¹⁻⁵ followed by β decay, such as the astrophysical r-process and nuclear weapons tests. Delayed-fission processes may also provide a sensitive probe of fission barriers in the heavy-element region.⁶

A. Theoretical considerations

The probability of this decay mode, P_{DF}, can be expressed experimentally as

$$P_{DF} = \frac{N_{if}}{N_i}, \tag{1}$$

where N_i is the number of the type of decays of interest (e.g., β or EC) and N_{if} is the number of those decays leading to delayed fission. P_{DF} can also be derived as

$$P_{DF} = \frac{\int_0^{Q_i} W_i(Q_i - E) \frac{\Gamma_f}{\Gamma_f + \Gamma_\gamma}(E) dE}{\int_0^{Q_i} W_i(Q_i - E) dE}, \tag{2}$$

where W_i(E) is the transition probability function for the decay of interest, Γ_f/(Γ_f+Γ_γ)(E) is the ratio of the fission width of excited levels within the daughter nucleus to the total depopulation width of these states, E is the excitation energy of the daughter nucleus, and Q_i is the Q value for the decay of interest.

The transition probability function W_i(E) can be expressed as the product of the Fermi function f and the beta strength function S_β giving

$$W_i(E) \approx f(Q_i - E, Z) S_\beta(E). \tag{3}$$

The Fermi function may be approximated as

$$f \approx \begin{cases} (Q_\epsilon - E)^2 & \text{for EC decay} \\ (Q_\beta - E)^5 & \text{for } \beta \text{ decay,} \end{cases} \tag{4}$$

for the calculation of P_{DF} in Eq. (2).

S_β can be treated in several different ways. It can be taken as being proportional to the nuclear level density,^{2,7} it can be generated from the gross theory of β decay,⁸ or it can be taken as a constant above a certain energy.^{9,10} Klapdor *et al.*¹¹ have pointed out that all three of these common techniques ignore low-lying structure in the beta strength function, S_β. Klapdor found inclusion of low-lying structure in the calculation of P_{DF} to have a significant impact on the value obtained.¹¹ However, for a qualitative understanding of P_{DF}, treating S_β as a constant above a cutoff energy is acceptable.

The large dependence of P_{DF} on the energy available for the decay and the structure of the fission barrier arises

from the fission-width term, $\Gamma_f/(\Gamma_f+\Gamma_\gamma)(E)$. Γ_γ , the width for gamma decay, can be estimated from the probability for γ transitions, P_γ as¹²

$$\Gamma_\gamma = \frac{P_\gamma}{2\pi\rho} = \frac{C_\gamma \Theta^4 e^{(E/\Theta)}}{2\pi\rho}, \quad (5)$$

where ρ is the nuclear level density, C_γ is a constant with the value $9.7 \times 10^{-7} \text{ MeV}^{-4}$, and Θ is the nuclear temperature (0.5–0.6 MeV). The fission width Γ_f can be derived from the penetrability of the fission barrier in a similar fashion, yielding

$$\Gamma_f = \frac{P_f}{2\pi\rho}, \quad (6)$$

where P_f is the penetrability of the fission barrier.

Since the fission barrier in the region of the actinide nuclei is reasonably complex, it is common^{12,13} to simplify the penetrability through the entire two-humped barrier by approximating P_f to be

$$P_f \approx P_A(E)R_B, \quad (7)$$

where $P_A(E)$ is the penetrability for tunneling through the inner barrier and R_B is the transmission coefficient for fission from the lowest state in the second well. This has the effect of requiring the nuclear motion in the second well to be strongly damped, i.e., not allowing fission from the second well to occur before γ decay to the lowest-lying state. This is a rather crude approximation (see, for example, Ref. 14) which is not valid at high energies, but it is appropriate at the excitation energies produced by delayed fission. As a result of this approximation, the calculation of P_f becomes much simpler. Transmission through the inner barrier B_A can then be approximated as a simple parabolic barrier problem using the Hill-Wheeler¹⁵ formalism

$$P_A = (1 + e^{2\pi(B_f - E)/h\omega_f})^{-1}, \quad (8)$$

where B_f is the height of the barrier and ω_f is the barrier curvature. This allows Γ_f to be expressed as

$$\Gamma_f \approx \frac{R_B}{2\pi\rho} (1 + e^{2\pi(B_f - E)/h\omega_f})^{-1}. \quad (9)$$

One can then express the quantity $\Gamma_f/(\Gamma_\gamma+\Gamma_f)(E)$ as

$$\frac{\Gamma_f}{\Gamma_\gamma + \Gamma_f}(E) \approx \frac{R_B (1 + e^{2\pi(B_f - E)/h\omega_f})^{-1}}{C_\gamma \Theta^4 e^{(E/\Theta)} + R_B (1 + e^{2\pi(B_f - E)/h\omega_f})^{-1}} \quad (10)$$

which illustrates the exponential dependence of this term in Eq. (2) on the energy available for decay and the structure of the fission barrier.

Utilizing these approximations, it is possible to rewrite Eq. (2) for electron capture in the following simplistic form,

$$P_{\text{DF}} \approx \frac{\int_C^{Q_\epsilon} (Q_\epsilon - E)^2 \frac{\Gamma_f}{\Gamma_\gamma + \Gamma_f}(E) dE}{\int_C^{Q_\epsilon} (Q_\epsilon - E)^2 dE}, \quad (11)$$

where C is the cutoff energy below which S_β is presumed to be zero. This value has been given¹⁰ as $C = 26A^{-1/2}$ MeV. The integral in the denominator is trivial, and may be evaluated directly to give a normalization function $N_\epsilon(A)$,

$$[N_\epsilon(A)]^{-1} \equiv \int_C^{Q_\epsilon} (Q_\epsilon - E)^2 dE = \frac{(Q_\epsilon - 26A^{-1/2})^3}{3}. \quad (12)$$

The remaining form of P_{DF} ,

$$P_{\text{DF}} \approx N_\epsilon(A) \int_C^{Q_\epsilon} (Q_\epsilon - E)^2 \frac{\Gamma_f}{\Gamma_\gamma + \Gamma_f}(E) dE, \quad (13)$$

is exponentially dependent on the difference between the fission barrier and the energy available for decay, the electron-capture Q value. Hence, for delayed fission to become a prominent decay mode in the actinide region (where fission barriers are on the order of 4–6 MeV), it is necessary to choose nuclei in which Q_ϵ is comparable to the fission barrier. This requires study of nuclei far from the valley of β stability, which introduces a number of experimental difficulties in the production and characterization of these nuclei.

Of course, it should be emphasized that the form of the delayed-fission probability P_{DF} developed in Eq. (13) is valid only for a qualitative understanding of the phenomenon of delayed fission. A quantitative model of P_{DF} would require a rigorous treatment of the structure of the beta strength function S_β as it appears in Eq. (3), no doubt including the low-lying structure¹¹ imposed on S_β by levels within the daughter nucleus. A quantitative model should also include treatment of transmission through realistic fission barriers and avoid the oversimplification of 100% damping required for the approximation in Eq. (7).

B. Experimental precedents

Fission tracks possibly resulting from EC-delayed fission (ϵDF) were first observed^{16,17} in the light americium and neptunium regions as early as 1966. In 1969, Berlovich and Novikov¹⁸ noted that the nuclei in question met the conditions required for delayed fission, although the observed fissions were not specifically attributed¹⁹ to delayed-fission processes until 1972. A fission activity, attributed to ϵDF in ^{232}Am , was reported by Habs *et al.*¹³ in 1978, and the P_{DF} for this isotope was reported to be on the order of one percent. An ϵDF branch has been tentatively assigned²⁰ to ^{242}Es , again with a P_{DF} on the order of one percent. Recently, ϵDF has been reported²¹ outside the actinide elements, in the region of ^{180}Hg .

Most studies to date have reported only half-life and fission cross-section (σ_f) data measured without any separation of the delayed-fissile species from other reaction products. The electron-capture cross section (σ_ϵ), when reported, has generally been extracted from theoretical calculations or systematics, not measured experimentally. ^{242}Es - ^{242}Cf is an exceptional case in that it was separated from most other reaction products using the velocity filter, SHIP, at GSI, but Hingmann *et al.*²⁰ were unable

to unambiguously identify the fissioning species. They were able, however, to measure the α particles emitted from the EC daughter ^{242}Cf and hence estimate σ_ϵ reasonably well. Gangrskii *et al.*¹² report delayed-fission probabilities for several transcurium nuclei using the measured α decay of the EC daughter to estimate σ_ϵ , providing the observed fission does arise from the assumed parent. All reports of ϵDF are summarized in Table I.

β -delayed fission (βDF) has been postulated to play a role in multiple neutron-capture processes since the 1950's. βDF was proposed by Burbidge, Burbidge, Fowler, and Hoyle¹ as a route for depleting the yield of heavy elements produced in supernovae. βDF is also one possible explanation of why superheavy elements are not found in nature.^{2,3} βDF had been predicted to significantly influence heavy-element yields in nuclear weapons tests;^{2,3} however, a recent reexamination of these data shows that the predicted delayed-fission effects are seriously overestimated.^{23,24}

The first report of an observed fission activity attributed to β -delayed fission appeared in 1978. ^{236}Pa and ^{238}Pa were reported by Gangrskii *et al.*²⁵ to exhibit βDF with delayed-fission probabilities of about 10^{-10} and $10^{-6.2}$, respectively. The experiment of Gangrskii *et al.* involved no chemical separation after producing the two protactinium isotopes. Subsequently, Baas-May *et al.*²⁶ studied ^{238}Pa using automated chemical separation procedures and observed no βDF from this isotope. They set an upper limit on the delayed-fission probability for ^{238}Pa of $P_{\text{DF}} \leq 2.6 \times 10^{-8}$. This failure to confirm βDF in ^{238}Pa cast considerable doubt on the earlier report²⁵ of a βDF branch in ^{236}Pa , since both ^{236}Pa and ^{238}Pa were measured in a similar fashion. ^{256m}Es is the most recently identified²⁷ β -delayed fissile species. ^{256m}Es is also the first case in which the fissioning isometric level in the daughter has been assigned. A summary of experimental reports of βDF is presented in Table II.

C. Selection of ^{234}Am

^{234}Am was selected for this study for several reasons. First, its reported¹⁹ half-life of 2.6 min is long enough to

allow multistep radiochemical procedures to be performed. With a judicious choice of procedures, an americium fraction could be purified sufficiently to allow observation of the K -capture x rays from the decay of ^{234}Am to ^{234}Pu without excessive γ interference. This would allow determination of the EC cross section experimentally, yielding half of the data required to determine P_{DF} by Eq. (1).

Secondly, ^{234}Am had been reported to have an ϵDF branch,¹⁹ although no value of P_{DF} was reported. However, using the systematic approach of Habs *et al.*¹³ and a Q_ϵ of 3.96 MeV for ^{234}Am (calculated using the masses of Möller, Myers, Świątecki, and Treiner²⁸), its P_{DF} could be estimated to be on the order of 10^{-4} to 10^{-5} . Since the $^{237}\text{Np}(\alpha, 7n)$ reaction can be used to produce ^{234}Am , the overall production cross section (σ_T) can be roughly estimated to be about 2 orders of magnitude larger than the $^{237}\text{Np}(\alpha, 9n)$ reaction employed by Habs *et al.*¹³ to produce ^{232}Am . This implies that the apparent fission production cross section ($\sigma_{\langle f \rangle}$), defined as

$$\sigma_{\langle f \rangle} = \sigma_T B_\epsilon P_{\text{DF}} \quad (14)$$

(where B_ϵ is the EC branching ratio), would be on the same order of magnitude as $\sigma_{\langle f \rangle}$ observed in the ^{232}Am study by Habs *et al.*,¹³ since the expected decrease in P_{DF} would be approximately balanced by the increase in σ_T . Furthermore, since the recent development²⁹ of the light ion multiple target system (LIM target system) allows the use of multiple targets, the fission production rate could be increased linearly with the number of targets irradiated. This would allow detection of a sufficient number of fissions to measure both the total kinetic energy (TKE) and mass-yield distributions of the ^{234}Am ϵDF mode.

Measurement of the TKE and mass-yield distributions is important because ϵDF allows the study of fission from nuclei with very low excitation energy.³¹⁻³⁴ This very low-energy mode is essentially inaccessible this far from stability with common techniques such as (n, f) and charged-particle reactions. Low excitation energy fission data may assist in understanding the dynamics of the

TABLE I. Summary of reported observations of EC-delayed fission. NR denotes "not reported."

Nuclide ^a	$t_{1/2}$ ^b	P_{DF} ^c	Reference
^{250}Md	52 s	2×10^{-4}	Gangrskii 1980 (12)
^{248}Es	28 min	3×10^{-7}	Gangrskii 1980 (12)
^{246}Es	8 min	3×10^{-5}	Gangrskii 1980 (12)
^{244}Es	37 s	10^{-4}	Gangrskii 1980 (12)
$^{242}\text{Es}?$	5-25 s	$(1.4 \pm 0.8) \times 10^{-2}$	Hingmann 1985 (20)
^{240}Bk	4 min	10^{-5}	Gangrskii 1980 (12)
^{234}Am	2.6 ± 0.2 min	NR	Skobelev 1972 (19)
^{234}Am	2.6 ± 0.2 min	NR	Somerville 1977 (22)
^{232}Am	1.4 ± 0.25 min	NR	Skobelev 1972 (19)
^{232}Am	0.92 ± 0.12 min	$1.3^{+4}_{-0.8} \times 10^{-2}$	Habs 1978 (13)
^{228}Np	60 ± 5 s	NR	Skobelev 1972 (19)
$^{180}\text{Tl}?$	$0.70^{+0.12}_{-0.09}$ s	$\sim 10^{-6}$	Lazarev 1987 (21)

^aThe parent nuclide undergoing EC decay to excited states in the daughter which then fission is given.

^bHalf-life is given as reported, or converted to a common unit when multiple references exist.

^cError limits are given if reported.

TABLE II. Summary of reported observations of β -delayed fission.

Nuclide ^a	$t_{1/2}$ ^b	P_{DF}	Reference
$^{256\text{m}}\text{Es}$	7.6 h	2×10^{-5}	Hall 1989 (27)
$^{238}\text{Pa}^{\text{c}}$	2.3 min	6×10^{-7}	Gangrskii 1978 (25)
$^{238}\text{Pa}^{\text{d}}$	2.3 min	$\sim 10^{-8}$	Gangrskii 1978 (25)
$^{238}\text{Pa}^{\text{e}}$	2.3 min	$\leq 2.6 \times 10^{-8}$	Baas-May 1985 (26)
$^{236}\text{Pa}^{\text{e}}$	9.1 min	$\sim 10^{-9}$	Gangrskii 1978 (25)
$^{236}\text{Pa}^{\text{f}}$	9.1 min	3×10^{-10}	Gangrskii 1978 (25)

^aThe parent nuclide undergoing β decay to excited states in the daughter which then fission is given.

^bHalf-life is given as reported, or converted to a common unit when multiple references exist.

^cProduced via $^{238}\text{U}(14.7\text{-MeV } n, p)$.

^dProduced via $^{238}\text{U}(8\text{-}20\text{-MeV } n, p)$.

^eProduced via $^{238}\text{U}(27\text{-MeV } \gamma, np)$.

^fProduced via $^{238}\text{U}(18\text{-MeV } d, \alpha)$.

fission process as the excitation energy of the fissioning nucleus goes to zero, leading to ground-state fission.

Also, the ^{234}Am ϵDF system is a nearly isotonic with nuclei displaying the ‘‘thorium anomaly,’’ i.e., triple-humped fission mass-yield distributions.^{35–38} Since ^{234}Am - ^{234}Pu may be in the transition region between the Th anomaly and ‘‘normal’’ double-humped mass-yield distributions, its fission properties may provide clues to understanding the Th anomaly. Indeed, delayed fission greatly expands the number of nuclei in the light actinide region whose fission properties may be studied, since nuclei such as ^{234}Pu have ground-state-fission half-lives which are too long relative to their overall half-lives to make studies of the ground-state-fission properties feasible.

II. EXPERIMENTAL

A. Targets and irradiation

Approximately 50 mg of ^{237}Np was chemically purified and dissolved as the nitrate in isopropanol to form a stock solution. An aliquot of this solution containing 150–250 μg of ^{237}Np was electrodeposited on 25- μm beryllium foil on a 1.23- cm^2 area for each target. Fifteen targets were made, with measured thicknesses ranging from 125 to 200 $\mu\text{g}/\text{cm}^2$. Each foil was mounted on a target holder frame. Twelve of the target holder frames were mounted in the LIM (Ref. 29) target system, with a spacing of approximately one centimeter between each target. A 25- μm beryllium foil served as the volume limiting foil for the LIM target system, and another 25- μm beryllium foil served as the vacuum window for the system.

The 75-MeV α -particle beam was provided by the Lawrence Berkeley Laboratory 88-inch cyclotron. The α -particle energy on the first target was 73.5 MeV, dropping to about 70 MeV after the last target in the stack. The beam intensity was 3–6 μA for all irradiations. The recoiling reaction products were collected on KCl aerosols in helium, which swept out the volume behind each target continuously. The activity-laden aerosols

were transported via a polyvinyl chloride capillary tube to either the rotating-wheel system (see Sec. II B below) or to a chemistry laboratory (see Sec. II C).

B. On-line measurements

For on-line measurements of the fission properties of ^{234}Am , the KCl aerosols were transported about five meters via a capillary tube and collected on a thin ($\approx 40 \mu\text{g}/\text{cm}^2$) polypropylene foil placed on the periphery of a wheel. At preset intervals, the wheel rotated 4.5° , passing the polypropylene foil through a series of six detector stations. The detector stations were placed so that the foil which had been in the aerosol collection position stepped immediately into station one, where it was counted for the preset interval. The foil subsequently passed through each detector station until it left station six, after which it was no longer counted. The wheel had 80 such foils along its perimeter, so at any given moment one sample could be collected while six others were being counted.

Each detector station consisted of a pair of ion-implanted passivated silicon detectors mounted above and below the plane of the wheel. This arrangement allowed detection of coincident fission fragments with an efficiency of approximately 60%. Each detector station could also detect α particles, again with a total efficiency of about 60%. Under the conditions of this experiment, the α -particle energy resolution was about 40 keV. The detectors were calibrated for the fission measurements with a ^{252}Cf source on a thin polypropylene foil.

The signals from the semiconductor detectors, after appropriate amplification and pulse shaping, were digitized to 11-bit (2048 channels) accuracy by Ortec AD-811 analog-to-digital converters (ADC's) in a CAMAC crate. These ADC's were controlled by a Standard Engineering CAMAC crate controller interfaced to a Digital Equipment Corporation LSI-11/73 computer system. As the data were collected, they were tagged with a time and a detector marker, and then written to magnetic tape in list (event-by-event) mode. Since each event has a time associated with it, the stepping interval of the wheel does not form the only time basis for half-life measurements. Subsequent sorting and histogramming was performed on the data to extract α spectra, fission-fragment spectra, coincidence data, and decay information. The rotating wheel is known as the ‘‘merry go-around’’ (MG), and the controlling computer system and its affiliated electronics are known as the realtime acquisition graphics system (RAGS), hence the acronym MG RAGS.

C. Chemical procedures

Two different chemical separations were performed on the reaction products of these irradiations. The first separation was designed to determine the elemental assignment of the fission activity; the second was used to produce an americium sample suitable for measurement of the plutonium K x rays from the EC decay of ^{234}Am . Measurement of the EC decay of ^{234}Am in conjunction with the ^{234}Am ϵDF would allow determination of P_{DF} experimentally.

1. Chemical procedure for elemental assignment

In the separation designed to assign the Z of the fissioning activity produced by 75-MeV α on ^{237}Np , the activity-laden aerosols were transported about five meters via a capillary tube and collected on a tantalum foil. The activity and KCl were then dissolved in 20 μL of 8M HNO_3 . The resulting solution was passed through a 1-mm \times 10-mm anion-exchange column (Bio-Rad AG 1-X8, 200-400 mesh). Under these conditions all trivalent actinides will pass through the column, while the higher valence actinides are adsorbed by the resin. The column was washed with $\sim 100 \mu\text{L}$ of 8M HNO_3 , and the eluant was collected on a tantalum foil, dried, flamed, and counted with a silicon surface barrier (SSB) detector for α particles and fissions. The column was then washed with $\sim 100 \mu\text{L}$ of 3M HCl -0.1M HF to elute neptunium and plutonium. This eluant was also collected on a tantalum foil, dried, flamed, and counted. A flow chart of this separation procedure is given in Fig. 1. Data from the SSB detectors were stored using RAGS. The total time required for this separation was about 90 s.

2. Chemical procedure for P_{DF} and σ_{ϵ} measurement

This separation procedure had to be more specific for americium since it was necessary to separate americium from highly γ -active fission products. High purity was achieved by using a stacked-column technique. In this technique, a single column is made with two types of resin packed sequentially into the column support. For this experiment, the column consisted of a 3-mm \times 50-mm column of cation-exchange resin (Bio-Rad AG-MP-50, 200-400 mesh) atop a 3-mm \times 10-mm column of anion-exchange resin (Bio-Rad AG1-X8, 200-400 mesh). Elution with concentrated HCl allowed americium to be separated from monovalent fission products, divalent fission products, and the lanthanides in the top portion of

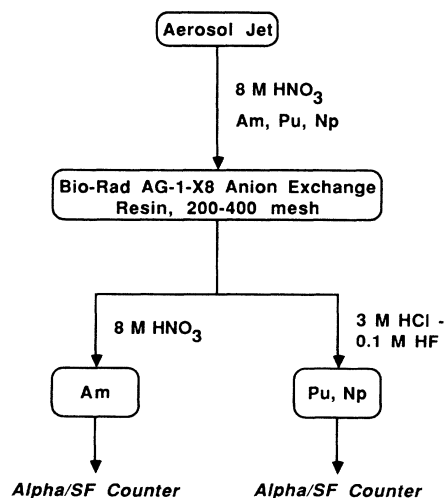


FIG. 1. Flow chart of the chemical separation used to confirm the assignment of the fission activity produced in the $^{237}\text{Np} + 75\text{-MeV } \alpha$ reaction to americium.

the column, and then plutonium and neptunium were adsorbed by the bottom portion of the column.

For this procedure, the activity was transported via capillary about 80 meters to a collection site in the chemistry laboratory at the LBL-88-inch cyclotron. The activity and KCl were dissolved in 20 μL of 0.5M HCl to which a known quantity of ^{241}Am ($t_{1/2} = 432a$) had been added as a yield tracer. The resulting solution was passed through the stacked column. Concentrated HCl was then passed through the column to remove americium. The fraction containing americium was collected, and americium was coprecipitated with CeF_3 . The precipitate was filtered, washed, and then counted with an intrinsic-germanium γ -spectroscopy system. A flow chart of this separation procedure is shown in Fig. 2. The total time required for this procedure was approximately four minutes. Signals from the germanium detector were pulse-height analyzed by an Ortec ACE-4K card in an IBM-PC compatible computer. A series of 1.0-min γ spectra were taken and saved on the PC's hard disk for subsequent analysis.

Fission from the ϵDF of ^{234}Am was measured on an alternating basis with the γ samples from the chemical separation. Samples for the fission measurements were produced by collecting the aerosols on a tantalum foil in the same collection apparatus as used in the chemical separations. The tantalum foil was flamed to red heat and counted in a windowless 2π gas flow proportional counter for ten minutes to measure the total number of fissions produced in a given collection. The efficiency of this detector for fissions was determined to be 98.6% with a calibrated ^{252}Cf source.

By measuring the fission production rate and the EC

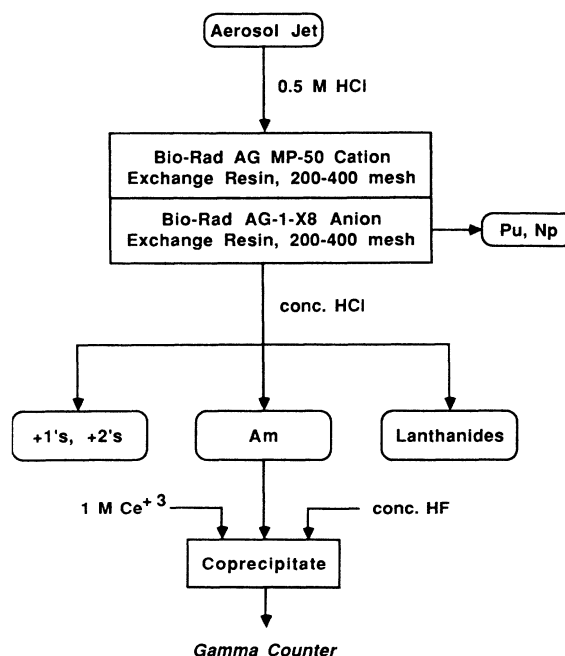


FIG. 2. Flow chart of the procedure used to isolate americium from the $^{237}\text{Np} + 75\text{-MeV } \alpha$ reaction in a form suitable for γ counting.

decay of ^{234}Am on an alternating basis, any unknown values cancel out in the calculation of P_{DF} provided these values oscillate more slowly than the rate of the experiments (six per hour). Therefore, values which would normally have to be estimated, such as gas-jet yield or effective target thickness, are removed from the calculation of P_{DF} . This increases the reliability of the measurement.

D. X-ray–fission correlation procedure

The time correlation between the K -capture x ray and the subsequent delayed fission was measured using aerosols collected directly without any chemical separation. The aerosols were collected on a tantalum foil for a suitable interval and the foil was placed before a light-tight transmission-mounted 300-mm² silicon surface barrier detector operated in air. In the initial experiments, the SSB detector and foil were sandwiched between two germanium γ detectors. In the final measurement, a NaI(Tl) γ detector was added to provide better timing resolution.

Since fission produces about ten prompt γ rays from the fission fragments,^{31,45} a high overall γ -detection efficiency would reject many of the true x-ray events by summing the x-ray pulse with a pulse arising from prompt γ rays. On the other hand, too low of an overall γ efficiency would also reduce the x-ray detection efficiency, and would hence reduce the observed correlation rate. By measuring the prompt γ rays from spontaneous fission in a source of ^{252}Cf , the spacing between the γ detectors and the sample was adjusted to bring the summing rejection level to 50%. As long as the γ multiplicity of the ^{234}Am ϵDF decay mode is not grossly different than that of ^{252}Cf , this would maximize the number of detected correlations. In the final configuration, each detector subtended a solid angle of about 6.7% of 4π . A 50% summing rejection level gives an overall correlation detection efficiency, using both germanium detectors, of 6.7% for each detected fission. The detector configuration is shown schematically in Fig. 3.

The signal from the SSB detector provided a common start for up to three electronic time-to-amplitude converters (TAC's). The stop signals for the first and second TAC's were provided by the first and second germanium

γ detectors, respectively, and the stop signal for the third TAC (in the last measurement) was provided by the NaI(Tl) detector. The time window on the TAC's was ± 500 ns. Calibrations were obtained using the prompt γ rays from the fission of ^{252}Cf and the γ rays in coincidence with the α particles from the decay of ^{249}Cf . The timing resolution of the germanium detectors was ~ 12 ns full width at half maximum (FWHM), and the energy resolution of these detectors was ~ 2 keV FWHM in the plutonium K x-ray region. The timing resolution of the NaI(Tl) detector was ~ 3 ns FWHM, and its energy resolution was ~ 30 keV FWHM in the 100-keV region. Upon detection of a fission event in the SSB detector, the amplitudes of the pulses (if any) in the SSB detector, the γ detectors, and the TAC's were recorded in list mode with RAGS. The times of the beginning of counting and the end of counting of each sample were also recorded on RAGS.

III. RESULTS AND DISCUSSION

A. Elemental assignment

Using the chemical procedure described in Sec. II C 1, 38 samples were processed and counted over about four hours. In each case, the aerosols were collected for three minutes and then subjected to the chemical separation. Each sample was counted for approximately 18 min. Twenty-seven fissions were observed in the americium fraction, and one was observed in the Np/Pu fraction. The one fission in the second fraction is consistent with the amount of americium expected to tail into this fraction. Prior tracer studies of this procedure had shown cross contamination of each fraction to be about 2%. The 6.46-MeV α group attributed³⁰ to ^{234}Am was also observed in the americium fraction.

Based on these results, we have assigned the fission activity produced in this reaction to americium (or the delayed fission to an americium precursor). The first fraction contains only the trivalent actinides produced in this reaction, while the second contains any neptunium, plutonium, protactinium, or thorium produced. Uranium would remain on the column in this procedure. Francium, radium, and actinium would follow the americium in this procedure, as would the lanthanides. However, the amount of Fr, Ra, and Ac produced in this reaction was observed (from the on-line α spectra) to be very small, and the lanthanides are unlikely to fission. Hence, americium is the only reasonable elemental assignment for the observed fission activity.

B. On-line results

The ϵDF and α -decay properties of ^{234}Am were measured over a forty hour irradiation using MG-RAGS as described in Sec. II B. The MG wheel was advanced one position every 2.50 min, so that the samples would spend approximately six half-lives between the six detector pairs. Each detector registered α particles and fissions for the full 2.50 min, except the first detector station. In the first station, signals from the α particles were suppressed for the first 12 s following the wheel motion. This allowed the $^8\text{B} + ^8\text{Li}$ ($t_{1/2} < 1$ s) α activity produced

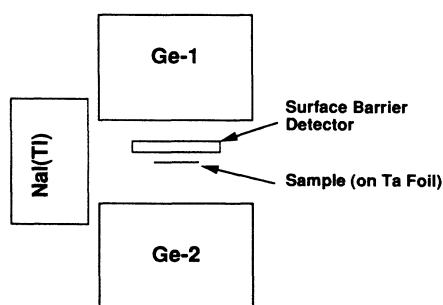


FIG. 3. Detector configuration of the x-ray–fission time-correlation experiment on ^{234}Am .

from the beryllium target backings to decay without causing excessive system deadtime. Fission signals from this detector were not seriously affected by these activities, and were analyzed for the full interval. After one full revolution of the wheel (80 positions), the wheel was replaced with a clean one so that any buildup of long-lived spontaneous fission activities was prevented.

1. Fission Properties

A total of 1188 coincident fission-fragment pairs was observed in these measurements. From these events, a more accurate value of the half-life was obtained than previously^{16,17,19,22} reported. The half-life was found to be 2.32 ± 0.08 min, slightly shorter than found in the previous reports. The decay curve for this fission activity is shown in Fig. 4. Each point on the decay curve has been normalized to represent the same number of samples per detector station. This is necessary since, for each wheel, the first station sees 80 foils before the acquisition is stopped while the second station sees 79, the third 78, and so on. The correction is fairly small (0% for the first station, rising to 12% for the last), but can significantly impact the measured half-life.

From the decay curve, we can estimate an apparent fission cross section for the ^{234}Am ϵDF mode from this reaction. The effective target thickness was estimated by extrapolating low-energy recoil ranges for the compound nucleus linearly to zero energy. Recoil ranges were taken from Northcliffe and Schilling,³⁹ and extrapolated when necessary. This method gave an estimate of the effective target thickness of $75 \mu\text{g}/\text{cm}^2$ per target. The efficiency of the aerosol-transport system was taken as 100%, although it could be lower. These assumptions result in an apparent fission cross section of about 0.2 nb.

Fission from ^{234}Am was observed to have a highly asymmetric mass distribution. The data were corrected for neutron emission with a neutron emission function $\bar{\nu}(A)$ similar to that of ^{252}Cf , normalized to $\bar{\nu}_T = 2.4$. Pre- and postneutron emission values are given in Table III. Table III lists two values for each property: the first column gives the results as calculated using the Schmitt, Kiker, and Williams (SKW) method⁴⁰ with the SKW calibration values for ^{252}Cf ; the second column gives the re-

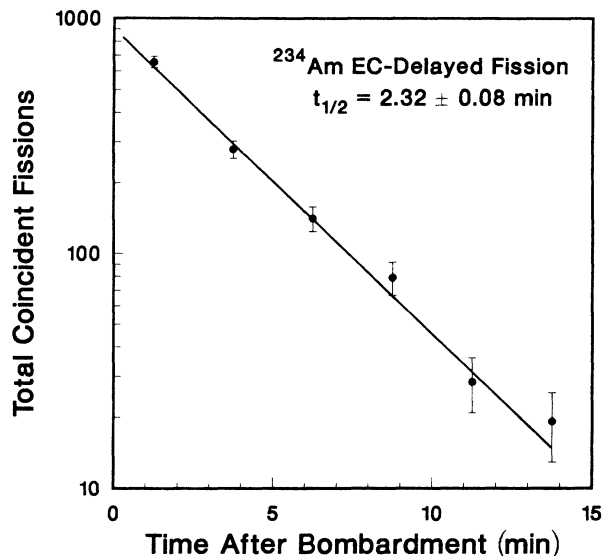


FIG. 4. Decay curve of the ^{234}Am EC-delayed fission activity as measured on MG RAGS. The wheel stepping time was 2.50 min.

sults as calculated using the SKW method with the energy calibration parameters of Weissenberger.⁴¹ The Weissenberger calibration values are more accurate than the SKW, but in order to compare the delayed-fission properties of ^{243}Am with previous data it was necessary to use the same calibration method as used for the previous data. Figure 5 shows the TKE and mass-yield distributions of the ^{234}Am ϵDF mode after corrections for neutron emission. The mass-yield distribution has a peak-to-valley ratio of 7 resulting from the asymmetric fission. The preneutron emission mass-yield distribution of an evaporated source of ^{252}Cf showed a peak-to-valley ratio of 5.6 under similar conditions. The TKE distribution is symmetric, and shows only one component. The behavior of the TKE and TKE as a function of mass fraction is shown in the TKE contour⁴² plot in Fig. 6. The TKE value of 175 MeV (SKW) for the ^{234}Am ϵDF is comparable to the predicted TKE (Refs. 43 and 44) for ground state fission from ^{234}Pu , as shown in Fig. 7.

The highly asymmetric mass division and symmetric

TABLE III. Summary of the fission characteristics of the ^{234}Am ϵDF mode.

	SKW ^a	Weissenberger ^b
Postneutron $\overline{\text{TKE}}$ ^c	173 \pm 5 MeV	171 \pm 5 MeV
Preneutron TKE	175 \pm 5 MeV	173 \pm 5 MeV
Postneutron $\overline{\text{KE}}$ ^d of high-energy fragment	99.8 \pm 2.0 MeV	98.6 \pm 2.0 MeV
Postneutron $\overline{\text{KE}}$ of low-energy fragment	73.5 \pm 1.4 MeV	72.3 \pm 1.5 MeV
Preneutron $\overline{\text{KE}}$ of high-energy fragment	100.6 \pm 2.0 MeV	99.4 \pm 2.0 MeV
Preneutron $\overline{\text{KE}}$ of low-energy fragment	74.1 \pm 1.4 MeV	72.9 \pm 1.5 MeV
Average mass of the light fission fragment	99.1 \pm 0.1	99.0 \pm 0.1
Average mass of the heavy fission fragment	134.8 \pm 0.1	135.0 \pm 0.1

^aCalculated using the Schmitt, Kiker, and Williams (SKW) (Ref. 40) method and reference values for ^{252}Cf .

^bCalculated using the SKW method and the reference values of Weissenberger (Ref. 41) for ^{252}Cf .

^cAverage total kinetic energy.

^dAverage kinetic energy.

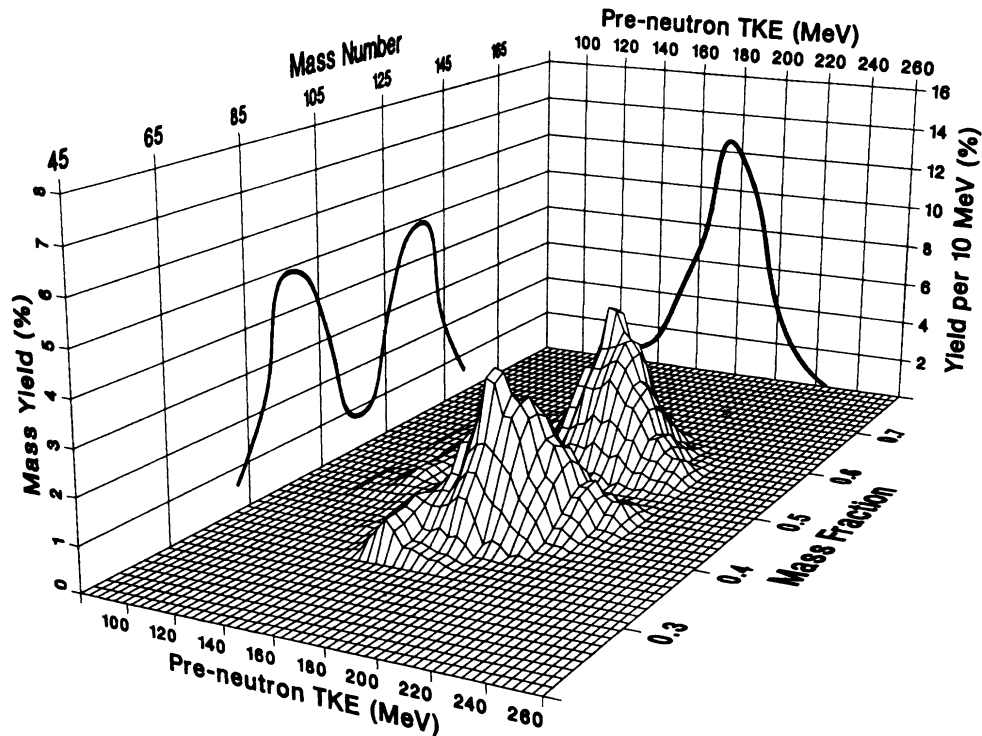


FIG. 5. Preneutron emission total kinetic energy (TKE) distribution of the ^{234}Am ϵDF mode and preneutron emission mass-yield distribution.

TKE distribution show no trace of the thorium anomaly. Therefore the transition region between “normal” double-humped mass distributions and the triple-humped distribution of the thorium anomaly must begin with lighter elements for this neutron number. Unfortunately, the lighter isotones have considerably smaller Q_ϵ values. This may reduce ϵDF in those nuclei to a level too low to measure their fission properties.

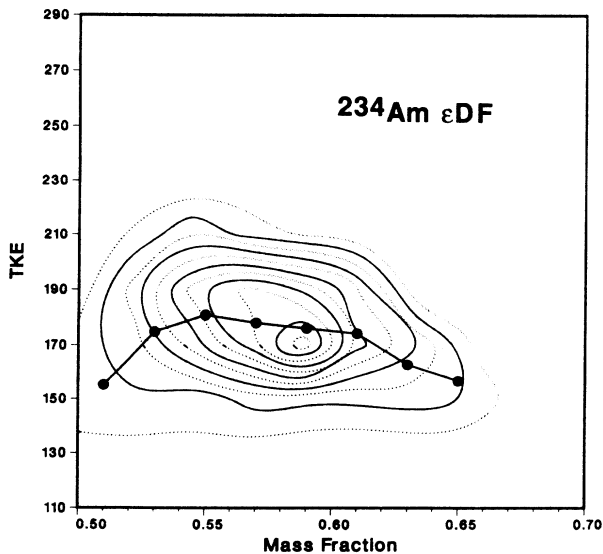


FIG. 6. Total kinetic energy and average total kinetic energy of ^{234}Am as a function of mass fraction.

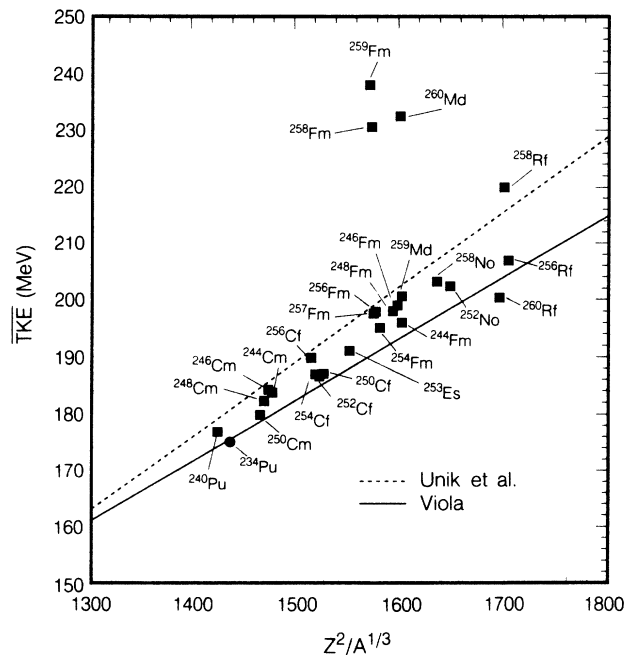


FIG. 7. Average total kinetic energy as a function of $Z^2/A^{1/3}$. The solid line is a linear fit of Viola (Ref. 43), and the dashed line is from Unik *et al.* (Ref. 44). Ground-state- (spontaneous) fission data for the *trans*-berkelium actinides are taken from Hoffman and Somerville (Ref. 45), and data for the lighter actinides are from Hoffman and Hoffman (Ref. 31). $Z^2/A^{1/3}$ for the ^{234}Am delayed fission is calculated for ^{234}Pu , since that is the fissioning nucleus. All data are based on the SKW (Ref. 40) method.

2. Alpha-decay properties

The 6.46-MeV α group³⁰ of ^{234}Am was observed in the on-line alpha spectra, along with a number of other peaks resulting from other reactions with the ^{237}Np target material, or with lead and bismuth impurities in the targets. An α spectrum from the MG, with the major groups identified, is shown in Fig. 8. Unfortunately, the large amount of short-lived β activity produced in this reaction reduced the α resolution of the first detector station to such a poor value that the α data from this detector station were omitted from the subsequent decay analysis.

The 6.46-MeV α peak was observed to decay with a two-component half-life, with one component about 2.3 min and the second too long for this experiment to measure accurately. After correction of the decay data to represent the same number of samples, half-life analysis was performed using the EXFIT (Ref. 46) computer code. The 2.32-min component is assigned to ^{234}Am . The long component is presumably due to tailing of the ^{211}Bi peak which contains growth from ^{211}Pb . The long component cannot be due to a long-lived isomeric state in ^{234}Am decaying by IT to the ground state. Such a state would also yield a long component in the delayed fissions, which was not observed. The decay of the 6.46-MeV α group is shown in Fig. 9. Comparison of the initial activities of the ^{234}Am α and ϵDF branches (from the on-line data) yields an alpha-to-fission ratio of 5.8 ± 0.4 . Using the same assumptions about effective target thickness and transport yields, the partial cross section for ^{234}Am produced by this reaction and decaying by alpha emission was found to be 1.1 nb.

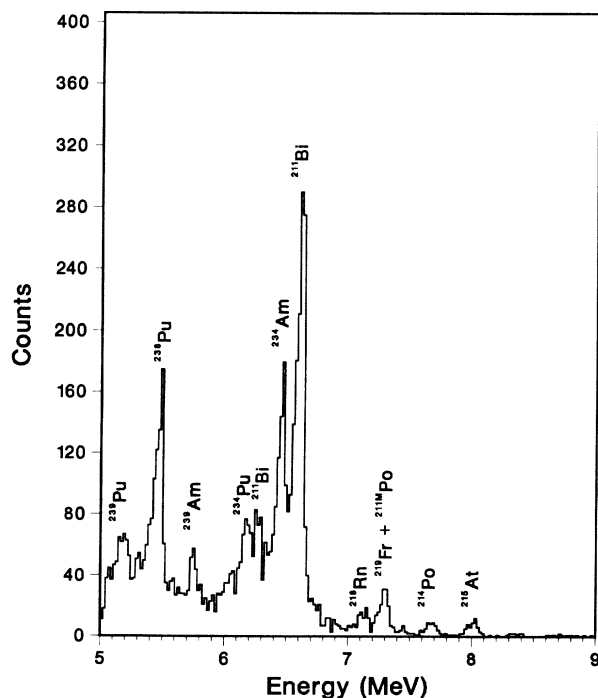


FIG. 8. Alpha spectrum from the on-line studies of ^{234}Am produced by the $^{237}\text{Np}(\alpha, xn)$ reaction and measured by the MG. This spectrum is taken from the second detector station, with a stepping time of 2.50 min. Major peaks are identified.

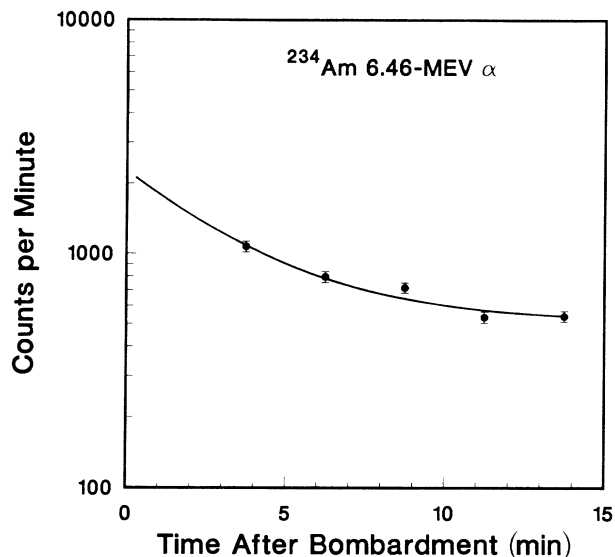


FIG. 9. Decay curve of the 6.46-MeV α group from the on-line α and fission measurements using the MG.

C. P_{DF} and σ_{ϵ} results

Americium fractions were repeatedly isolated chemically over an irradiation period of about four hours. Fission measurements were made in the same period on an alternating basis with the chemical separations. The chemically purified americium samples were γ counted repeatedly for approximately 40 min each. The fission samples were counted for one 10 min period each in the

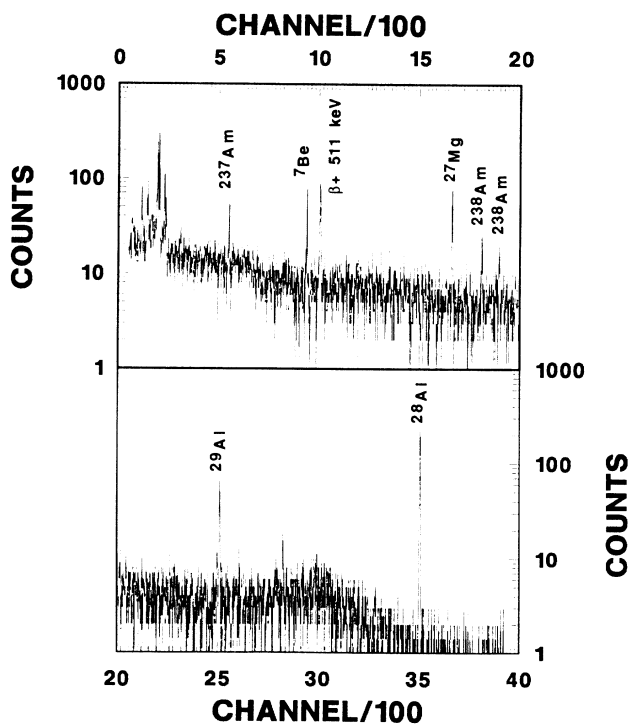


FIG. 10. Gamma rays in the range of 0–2 MeV observed in a chemically purified sample of americium. The K x-ray region is expanded and shown in Fig. 11.

proportional counter, and the integrated fissions were recorded. The γ spectra were analyzed using the SAMPO (Ref. 47) computer code, and half-life analysis was performed with the CLSQ (Ref. 48) code.

Figure 10 shows the γ rays observed in a representative spectrum from this experiment. Some ^{237}Am and ^{238}Am was visible within the spectra, probably produced by stripping reactions. A small amount of ^7Be , which was produced from the target backings, followed by the americium, as did small amounts of $^{28,29}\text{Al}$ and ^{27}Mg . The aluminum and magnesium were mostly likely produced by scattered beam on the aluminum target-holder cards. Half-life analysis confirmed the assignment of these peaks.

The K x-ray region from the spectrum used for Fig. 10 is expanded and shown in Fig. 11. The plutonium x rays resulting from the electron capture of americium are clearly visible. The only other peaks in this region are lead K x rays and the 59.5-keV γ ray from the ^{241}Am yield tracer.

Half-life analysis of the Pu K x rays revealed a two-component decay curve, with one component being short (about 2–3 min), and the other on the order of an hour. The long component was a mixture of the ^{237}Am ($t_{1/2}=73$ min) and ^{238}Am ($t_{1/2}=1.63$ h), and the short was ^{234}Am . The K x rays were fitted with two components using CLSQ, with the short component being set at 2.32 min and the long component allowed to vary. An example of such a fit is shown in Fig. 12. The resulting initial activities of the ^{234}Am electron-capture decay mode were corrected for detector efficiency, chemical yield, and K -fluorescence yield [taken as 97.7% (Ref. 49)]. The resulting initial disintegration rates were used for the calculation of σ_ϵ and P_{DF} .

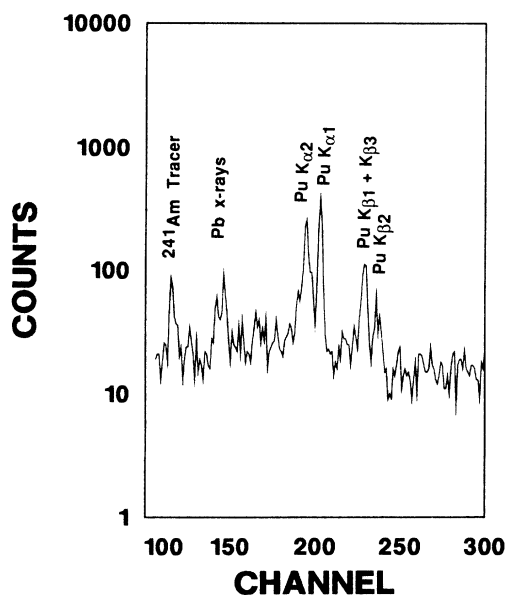


FIG. 11. The K x-ray region of the gamma spectrum of a chemically purified ^{234}Am sample.

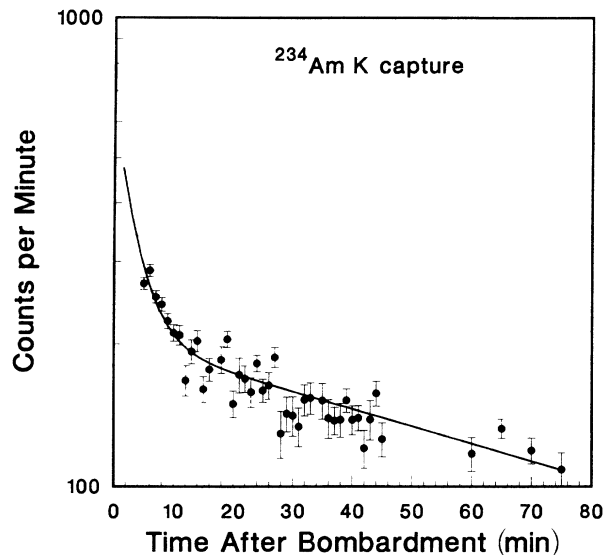


FIG. 12. Half-life fit for the plutonium K x rays observed from the chemically purified ^{234}Am sample.

The electron-capture cross section was calculated based on the following assumptions. First, the target thickness was estimated the same way as for the apparent fission cross section, yielding an effective total target thickness of $12 \times 75 \mu\text{g}/\text{cm}^2 = 900 \mu\text{g}/\text{cm}^2$. Second, the gas-jet yield was assumed to be 100%. Third, because of the lack of discernible γ lines in the spectrum with a 2.32-min half-life, it was assumed that the level density of the daughter was high enough that deexcitation proceeded through a series of high-energy (500–1000 keV) low-multipolarity transitions. Based on this assumption, the K x-ray production from internal conversion was taken as negligible. Of course, the last few transitions should be more highly converted, but without detailed information about the level scheme of ^{234}Pu any estimates on K conversion would be near baseless. With the above assumptions, σ_ϵ was determined to be $5.4 \pm 1.3 \mu\text{b}$ at the 1 σ (68%) confidence level.

The delayed-fission probability was calculated from the electron-capture initial activities and the number of fissions observed in the subsequent fission sample. By measuring each quantity nearly simultaneously, experimental variables such as the target thickness, the beam flux (since our flux was held at a constant $7 \text{ e}\mu\text{A}$ throughout this measurement, with less than 5% deviation), and the gas-jet yield should all cancel out. This allows us to calculate P_{DF} with a variant of Eq. (1),

TABLE IV. Individual P_{DF} determinations for ^{234}Am . P_{DF} was calculated in each case by Eq. (15).

$D_{0,\epsilon}$	I_f	$P_{\text{DF}}/10^{-5}$
$16\,694 \pm 13\%$	4	7.17
$15\,502 \pm 15\%$	4	7.74
$15\,157 \pm 12\%$	4,3	6.93
$11\,606 \pm 20\%$	3	7.74
$18\,929 \pm 17\%$	2	3.18
$19\,636 \pm 16\%$	5	7.65

$$P_{DF} = \frac{\lambda I_f / (e^{-\lambda t_1} - e^{-\lambda(t_1+t_C)})}{D_{0,\epsilon}}, \quad (15)$$

where λ is the decay constant for ^{234}Am , I_f is the number of fissions observed in a counting time t_C , t_1 is the time from end of bombardment to the start of the fission counting, and $D_{0,\epsilon}$ is the initial activity for electron capture. Employing this relationship, P_{DF} was calculated and averaged over all of the separate determinations. This yielded a value of P_{DF} of $(6.6 \pm 1.8) \times 10^{-5}$ at the 1σ (68%) confidence level. Table IV lists the individual values obtained.

Using the delayed-fission probability as the ratio of fissions to EC decays and the α -to-fission ratio determined in Sec. III B 2 above, the α -to-EC ratio was found to be $(3.9 \pm 1.2) \times 10^{-4}$.

D. X-ray–fission results

Samples were collected from the gas-jet system every four minutes and then placed in the counting chamber for the correlation studies. Approximately 1500 samples were processed in this manner. The gross γ rate of the samples was approximately 10^3 counts per second (detected), so less than 0.1% of the fissions would be expected to be in coincidence with background γ rays because of the narrow timing window. Figure 13(a) shows the x-ray and γ spectrum of those events in prompt coincidence with the fission signal. Figure 13(c) is the logarithm of a maximum-likelihood fit L of an idealized x-ray spectrum [shown in Fig. 13(b)] to the observed data. The number of counts expected in channel i , Y_i , is given by

$$Y_i = \left[\sum_{j=1}^5 \frac{A_j}{\sigma\sqrt{2\pi}} e^{-(i-C_j)^2/2\sigma^2} \right] + B_i, \quad (16)$$

where σ represents the Gaussian width of the detector response, A_j and C_j are the number of expected counts and centroid in the j th peak of the K x-ray multiplet, respectively, and B_i is the expected background in channel i . The probability of observing Z_i counts in channel i when Y_i counts are expected is given by a Poisson distribution,

$$P_i = \frac{Y_i^{Z_i} e^{-Y_i}}{Z_i!}, \quad (17)$$

and the likelihood function is given as the product of all the probabilities,

$$L = \prod_i P_i. \quad (18)$$

In Fig. 13(c), the logarithm of the likelihood is plotted as a function of the $K_{\alpha 1}$ position of the ideal spectrum. From the likelihood functions, the most probable $K_{\alpha 1}$ energy was found to be 103.6 ± 0.5 keV, in excellent agreement with the plutonium $K_{\alpha 1}$ energy of 103.76 keV. The total number of K x rays was found to be 32 ± 6 by allowing the intensity of the ideal spectrum (Y) to vary within the maximum-likelihood analysis. Observed and expected x-ray intensities for plutonium are given in Table V.

No evidence was observed for fission delay times longer than the best timing resolution of these experiments, about 3 ns. The fact that plutonium x rays can be seen requires that the lifetime of the fissioning state be longer than the time it takes the orbital electrons to cascade down and fill a K vacancy. The time required for this is on the order of 10^{-17} s.⁵⁰ We can therefore set boundaries on the excited half-life of 10^{-8} ns $< t_{1/2} < 3$ ns. If the nucleus is truly 100% damped in the second well [as it was assumed in Eq. (7)], then these limits are also limits on the lifetime of the shape isomer ^{234f}Pu . These limits are consistent with the half-life systematics of plutonium shape isomers (see Fig. 3 of Ref. 51), from which one would expect the half-life of ^{234f}Pu to be in the range of 1–100 ps.

The coincidence γ data in Fig. 13 also show what appear to be true peaks at about 112, 147, 168, and 185 keV. These peaks are very weak, but prompt γ rays from fission fragments do not display such structure. It is pos-

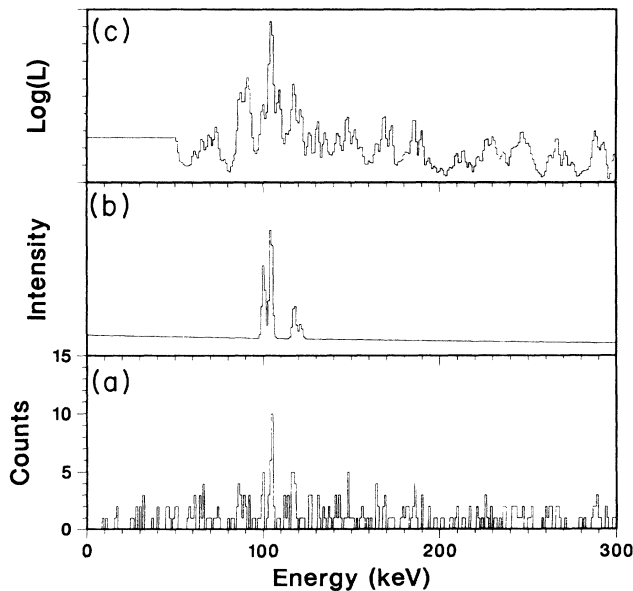


FIG. 13. X-ray–fission correlation results. (a) X rays and γ rays in coincidence with delayed fission from ^{234}Am . (b) An idealized plutonium K x-ray spectrum, based on the measured detector resolution and an expected prompt γ -ray continuum. (c) The likelihood function for the position of the ideal spectrum (b) in the data (a), as a function of the $K_{\alpha 1}$ position.

TABLE V. Observed and expected x-ray intensities from the correlated x-ray–fission data. Expected x-ray intensities are taken from the *Table of Isotopes* (Ref. 49).

X-ray	E/keV	I_{theo}	No. observed ^a	I_{obs}
$\text{Pu}K_{\alpha 2}$	99.55	0.299	10	0.20 ± 0.07
$\text{Pu}K_{\alpha 1}$	103.76	0.479	22	0.45 ± 0.12
$\text{Pu}K_{\beta 1'}$	116.9	0.162	14	0.29 ± 0.09
$\text{Pu}K_{\beta 2'}$	120.6	0.060	3	0.06 ± 0.04

^aApproximately 18 of the observed events are attributable to the prompt γ -ray continuum.

sible that these γ rays are a result of the level structure of ^{234}Pu in the second well. If this is the case, the correlation of these γ rays supports the hypothesis that the second well is strongly damped. Unfortunately, the poor statistics of the γ - γ -fission-time correlation data precludes constructing a level scheme for ^{234f}Pu .

The observation of x-ray-fission correlations in this experiment unequivocally proves that the decay is indeed EC-delayed fission. This is the first ϵDF process for which direct proof has been obtained.⁵² The only other time-correlated proof of a delayed-fission process is for βDF in ^{256m}Es .²⁷

IV. CONCLUSIONS

^{234}Am was produced using multiple ^{237}Np targets irradiated with α particles in the energy range 70.0–73.5 MeV. The half-life was determined as 2.32 ± 0.08 min using the MG-RAGS rotating-wheel system at the Lawrence Berkeley Laboratory 88-inch cyclotron. The fission properties of the ^{234}Am ϵDF mode were measured. It was found to have a highly asymmetric mass division. The total kinetic energy distribution displayed only one component, and had an average TKE of 173 ± 5 MeV. The mass-yield distribution showed no evidence of the thorium anomaly observed in lighter Z nuclei with the same neutron number. These are the first reported measurements of the fission properties of a delayed-fissile nucleus.

The ϵDF mode provided a mechanism for studying the fission properties of a nucleus far from stability near its ground state. No other technique exists which would allow the study of near-ground-state fission from a specific nucleus this far from β stability.

TABLE VI. Summary of cross sections determined in this work. All cross sections were calculated assuming a 100% gas-jet yield.

σ_{ϵ}	$5.4 \pm 1.3 \mu\text{b}$
σ_f	$\sim 0.2 \text{ nb}$
σ_{α}	$\sim 1.1 \text{ nb}$

The electron-capture branch of ^{234}Am was measured radiochemically, yielding a cross section of $5.4 \pm 1.3 \mu\text{b}$ for the $^{237}\text{Np}(\alpha, 7n)$ reaction. The delayed-fission probability was measured experimentally, and found to be $(6.6 \pm 1.8) \times 10^{-5}$. The 6.46-MeV α decay of ^{234}Am was found to have a branching ratio of $(3.9 \pm 1.2) \times 10^{-4}$. This report is also the first time both the fission and the EC branch leading to the fission have been directly measured. The cross sections reported in this work are summarized in Table VI.

Finally, the coincidence data between the plutonium x ray and the fission provide direct proof that the fissions observed in this experiment are the result of americium K capture followed by fission of excited states in the daughter plutonium nucleus. These data confirm⁵² that ϵDF is a decay mode of ^{234}Am .

ACKNOWLEDGMENTS

The authors wish to thank the staff and crew of the Lawrence Berkeley Laboratory 88-inch cyclotron for their assistance. This work was supported in part by the U.S. Department of Energy under Contract DE-AC03-76SF00098 and in part by a National Science Foundation Graduate Fellowship.

*Present address: Nuclear Chemistry Division L-396, Lawrence Livermore National Laboratory, Livermore, CA 94550.

†Present address: Forensics Division, Orange County Sheriff's Department, 601 North Ross, Santa Ana, CA 92701.

¹E. M. Burbidge, G. R. Burbidge, W. A. Fowler, and F. Hoyle, *Rev. Mod. Phys.* **29**, 547 (1957).

²C.-O. Wene and S. A. E. Johansson, *Phys. Scr.* **10A**, 156 (1974).

³C.-O. Wene, *Astron. Astrophys.* **44**, 233 (1975).

⁴H. V. Klapdor, T. Oda, J. Metzinger, W. Hillebrandt, and F. K. Thielman, *Z. Phys. A* **299**, 213 (1981).

⁵B. S. Meyer, W. M. Howard, G. J. Matthews, K. Takahashi, P. Möller, and G. Leander, *Phys. Rev. C* **39**, 1876 (1989).

⁶Yu. A. Lazarev, Yu. Ts. Oganessian, and V. I. Kuznetsov, Joint Institutes for Nuclear Research, Dubna, Report No. JINR-E7-80-719, 1980.

⁷S. Shalev and G. Rudstam, *Nucl. Phys.* **A275**, 76 (1977).

⁸T. Kodama and K. Takahashi, *Nucl. Phys.* **A239**, 489 (1975).

⁹P. Hornshøj, B. R. Erdal, P. G. Hansen, B. Jonson, K. Aleklett, and G. Nyman, *Nucl. Phys.* **A239**, 15 (1975).

¹⁰K. L. Kratz and G. Herrmann, *Z. Phys.* **263**, 435 (1973).

¹¹H. V. Klapdor, C.-O. Wene, I. N. Isosimov, and Yu. W. Naumov, *Z. Phys. A* **292**, 249 (1979).

¹²Yu. P. Gangrskii, M. B. Miller, L. V. Mikhailov, and I. F. Kharisov, *Yad. Fiz.* **31**, 306 (1980) [*Sov. J. Nucl. Phys.* **31**, 162 (1980)].

¹³D. Habs, H. Klewe-Nebenius, V. Metag, B. Neumann, and H. J. Specht, *Z. Phys. A* **285**, 53 (1978).

¹⁴U. Goerlach, D. Habs, M. Just, V. Metag, P. Paul, H. J. Specht, and H. J. Maier, *Z. Phys. A* **287**, 171 (1978).

¹⁵D. L. Hill and J. A. Wheeler, *Phys. Rev.* **89**, 1102 (1953).

¹⁶V. I. Kuznetsov, N. K. Skobelev, and G. N. Flerov, *Yad. Fiz.* **4**, 279 (1966) [*Sov. J. Nucl. Phys.* **4**, 202 (1967)].

¹⁷V. I. Kuznetsov, N. K. Skobelev, and G. N. Flerov, *Yad. Fiz.* **5**, 271 (1967) [*Sov. J. Nucl. Phys.* **5**, 191 (1967)].

¹⁸É. E. Berlovich and Yu. P. Novikov, *Dokl. Akad. Nauk SSSR* **185**, 1025 (1969) [*Sov. Physics—Dokl.* **14**, 349 (1969)].

¹⁹N. K. Skobelev, *Yad. Fiz.* **15**, 444 (1972) [*Sov. J. Nucl. Phys.* **15**, 249 (1972)].

²⁰R. Hingmann, W. Kuehn, V. Metag, R. Novotny, A. Ruckelshausen, H. Stroehrer, F. Hessberger, S. Hofmann, G. Muenzenberger, and W. Reisdorf, Gesellschaft für Schwerionenforschung, Darmstadt, Report No. GSI 85-1, 1985.

²¹Yu. A. Lazarev, Yu. Ts. Oganessian, I. V. Shirokovsky, S. P. Tretyakova, V. K. Utyonkov, and G. V. Buklanov, *Europhys. Lett.* **4**, 893 (1987).

²²L. P. Somerville, A. Ghiorso, M. J. Nurmi, and G. T. Seaborg, Lawrence Berkeley Laboratory Nuclear Science Division Annual Report, 1976–1977, Report No. LBL-6575, 1977.

²³R. W. Hoff, in *Weak and Electromagnetic Interactions in Nu-*

- clei*, edited by H. V. Klapdor (Springer-Verlag, Heidelberg, 1986), p. 207.
- ²⁴R. W. Hoff, Inst. Phys. Conf. Ser. No. 88/J. Phys. G: Nucl. Phys. **14**, Suppl., S343 (1986).
- ²⁵Yu. P. Gangrskii, G. M. Marinescu, M. B. Miller, V. N. Samoyusk, and I. F. Kharisov, Yad. Fiz. **27**, 894 (1978) [Sov. J. Nucl. Phys. **27**, 475 (1978)].
- ²⁶A. Baas-May, J. V. Kratz, and N. Trautmann, Z. Phys. A **322**, 457 (1985).
- ²⁷H. L. Hall, K. E. Gregorich, R. A. Henderson, D. M. Lee, D. C. Hoffman, M. E. Bunker, M. M. Fowler, P. Lysaght, J. W. Starnner, and J. B. Wilhelmy, Phys. Rev. C **39**, 1866 (1989).
- ²⁸P. Möller, W. D. Myers, W. J. Świątecki, and J. Treiner, At. Data Nucl. Data Tables **39**, 225 (1988).
- ²⁹H. L. Hall, M. J. Nurmia, D. C. Hoffman, Nucl. Instrum. Methods A **276**, 649 (1989).
- ³⁰Y. A. Ellis-Akovali, Nucl. Data Sheets **40**, 523 (1983).
- ³¹D. C. Hoffman and M. M. Hoffman, Annu. Rev. Nucl. Sci. **24**, 151 (1974).
- ³²H. J. Specht, Rev. Mod. Phys. **46**, 773 (1974).
- ³³H. J. Specht, Phys. Scr. **10A**, 21 (1974).
- ³⁴R. Vandenbosch and J. R. Huizenga, *Nuclear Fission* (Academic, New York, 1973).
- ³⁵E. Konecny, H. J. Specht, and J. Weber, Phys. Lett. **45B**, 329 (1973).
- ³⁶J. Blons, C. Mazur, D. Paya, M. Ribrag, and H. Weigmann, Nucl. Phys. A **414**, 1 (1984).
- ³⁷M. G. Itkis, V. N. Okolovich, and A. Ya. Rusanov, Fiz. Elem. Chastits At. Yadra **19**, 701 (1988) [Sov. J. Part. Nucl. **19**, 301 (1988)].
- ³⁸B. S. Bhandari and A. S. Al-Kharam, Phys. Rev. C **39**, 917 (1989).
- ³⁹L. C. Northcliffe and R. F. Schilling, Nucl. Data Tables A **7**, 233 (1970).
- ⁴⁰H. W. Schmitt, W. E. Kiker, and C. W. Williams, Phys. Rev. **137**, B837 (1965).
- ⁴¹E. Weissenberger, P. Geltenbort, A. Oed, F. Gönnerwein, and H. Faust, Nucl. Instrum. Methods A **248**, 506 (1986).
- ⁴²R. Brandt, S. G. Thompson, R. C. Gatti, and L. Phillips, Phys. Rev. **131**, 2617 (1963).
- ⁴³V. Viola, Nucl. Data, Sect. B **1**, 391 (1966).
- ⁴⁴J. P. Unik, J. E. Gindler, L. E. Glendenin, K. F. Flynn, A. Gorski, and R. K. Sjoblom, in *Proceedings of the 3rd IAEA Symposium on the Physics and Chemistry of Fission, 1973* (International Atomic Energy Agency, Vienna, 1974), Vol. 2, p. 19.
- ⁴⁵D. C. Hoffman and L. P. Somerville, in *Charged Particle Emission from Nuclei*, edited by D. N. Poenaru and M. Ivaşcu (CRC, Boca Raton, 1989), Vol. III, p. 1.
- ⁴⁶K. E. Gregorich, Ph.D. thesis (1985); also, Lawrence Berkeley Laboratory Report No. 20192, 1985.
- ⁴⁷J. T. Routti and S. G. Prussin, Nucl. Instrum. Methods **72**, 125 (1969).
- ⁴⁸J. B. Cumming, NAS-NS 3107, 25 (1963); also, Brookhaven National Laboratory Report No. BNL-6470, 1963.
- ⁴⁹C. M. Lederer, V. M. Shirley, E. Browne, J. M. Dairiki, R. E. Doebler, A. A. Shihab-Eldin, L. J. Jardine, J. K. Tuli, and A. B. Buyrn, *Table of Isotopes*, 7th ed. (Wiley, New York, 1978).
- ⁵⁰J. H. Scofield, At. Data Nucl. Data Tables **14**, 121 (1974).
- ⁵¹D. N. Poenaru, M. S. Ivaşcu, and D. Mazilu, in *Charged Particle Emission from Nuclei*, edited by D. N. Poenaru and M. Ivaşcu (CRC, Boca Raton, 1989), Vol. III, p. 41.
- ⁵²H. L. Hall, K. E. Gregorich, R. A. Henderson, C. M. Gannett, R. B. Chadwick, J. D. Leyba, K. R. Czerwinski, B. Kadkhodayan, S. A. Kreek, D. M. Lee, M. J. Nurmia, and D. C. Hoffman, Phys. Rev. Lett. **63**, 2548 (1989).